Letter

Optimal quantum Feshbach engines

Aaron Wandhammer, Vincent Hardel, Paul-Antoine Hervieux, and Giovanni Manfredi*
University of Strasbourg, CNRS, Institut de Physique et Chimie des Matériaux de Strasbourg, UMR 7504, 67034 Strasbourg, France

(Received 26 May 2026; accepted 9 September 2026; published 14 October 2026)

We develop a general optimization framework for high-efficiency quantum cycles implemented with a trapped Bose-Einstein condensate, whose control parameters are the trap stiffness and the interaction strength, the latter tuned via Feshbach resonance. Combining a variational description of the condensate dynamics with Nelson's stochastic quantization, we map the quantum evolution onto an effective classical Ornstein-Uhlenbeck process, enabling the systematic optimization of each cycle stroke. The optimal protocol is obtained by minimizing a user-defined cost functional that selects the best trade-off between protocol duration and arbitrary physical constraints (such as the expended work or the proximity to an adiabatic evolution). The resulting protocols remain remarkably stable over repeated cycles, demonstrating the robustness of the optimization strategy. More generally, our framework provides a systematic route to the optimal control of nonlinear Schrödinger equations, with potential applications to quantum fluids, nonlinear optics, and quantum plasmas.

DOI: 10.1103/ymmx-hskw

Introduction. The precise control of quantum matter is a central challenge in modern quantum physics, as it underpins the development of emerging quantum technologies [1,2]. The most reliable way to transfer a quantum system between states in a stable manner is through adiabatic transitions. Such transitions, however, require theoretically infinite time to maintain perfect stability throughout the evolution. Consequently, adiabatic protocols are often impractically slow for experimental applications. To overcome this limitation, the field of shortcuts to adiabaticity (STAs) has emerged [3,4]. Shortcuts to adiabaticity encompass a broad set of techniques, ranging from inverse engineering [5,6] and counteradiabatic driving [7,8] to fast-forward approaches [9], which enable finite-time transitions while reproducing the outcome of an adiabatic evolution. These methods provide experimentally robust protocols that steer the quantum system toward a stable final state by manipulating some control parameter. Despite two decades of progress, STA remain a topical area of research [10,11].

Recently, a novel STA technique was introduced [12], based on a quantum-classical analogy derived from Nelson's formulation of quantum mechanics [13], which recasts the Schrödinger equation as a classical stochastic process. Here we use this approach to control the dynamics of a Bose-Einstein condensate (BEC) confined in a cigar-shaped harmonic trap [14,15]. For ultracold atomic gases, the interaction strength is characterized by the scattering length a, which can be tuned with an external magnetic field that acts on the Feshbach resonance [16–19]. This tunability provides an additional control parameter, alongside the trap stiffness [20], for driving quantum state transitions. STA methods tailored to BECs with tunable interactions thus hold significant promise, notably in the development of quantum engines based on ultracold atomic gases [21–29].

Using Nelson's stochastic quantization, we first derive faster-than-adiabatic quantum protocols inspired by classical protocols originally developed for overdamped stochastic systems. We then develop optimal quantum protocols and optimal quantum cycles (engines) by exploiting the tunability of both the trap stiffness and the scattering length of the BEC.

Compared to other STA techniques [21,29], our method enables the construction of protocols that are optimal with respect to a cost functional freely specified by the user. This flexibility allows one to identify the best trade-off between, for instance, the protocol duration, the expended work, or the proximity to an adiabatic evolution. Under realistic conditions, this approach leads to a significant increase in the efficiency and generated power of a quantum engine based on a BEC.

Model. We consider a BEC confined in an elongated harmonic trap, where the longitudinal trapping frequency (along the x axis) is much smaller than the transverse one, $\omega_x \equiv \omega \ll \omega_\perp$, making the system quasi-one-dimensional [30,31]. In the mean-field approximation, the evolution of the condensate is governed by the Gross-Pitaevskii equation (GPE)

$$i\hbar\frac{\partial\psi}{\partial t} = \left(-\frac{\hbar^2}{2m}\nabla^2 + \frac{1}{2}m\omega^2x^2 + g_{1D}N|\psi|^2\right)\psi, \quad (1)$$

where $\psi(x,t)$ is the condensate wave function, $g_{1D} = 2a\hbar\omega_\perp$ is the effective one-dimensional coupling constant, a is the three-dimensional (3D) scattering length, and N is the number of atoms in the BEC. For simplicity, hereafter we write $g \equiv g_{1D}$ and define the trap stiffness as $\kappa \equiv m\omega^2$. Here the purpose is to steer the evolution of the BEC by acting on the stiffness of the trap $\kappa(t)$ and/or the interaction strength $g(t)$.

*Contact author: giovanni.manfredi@ipcms.unistra.fr

 ©2026 American Physical Society

To obtain an approximate solution of the GPE, we write the wave function as $\psi(x,t) = \sqrt{P(x,t)}e^{iS(x,t)}$ and assume that the density P is Gaussian and the phase S is quadratic in x, i.e., $P(x,t) = \frac{1}{\sqrt{2\pi}\sigma(t)}e^{-x^2/2\sigma^2(t)}$ and $S(x,t) = \alpha(t)x^2$. We then use a variational approach to determine the Gaussian wave function that is closest to the exact solution of the GPE [32,33]. This variational method yields the time dependence of the functions $\sigma(t)$ and $\alpha(t)$. For the latter, we get $\alpha(t) = \frac{m}{2\hbar}\frac{\dot{\sigma}}{\sigma}$, where the overdot denotes time differentiation. The width $\sigma(t)$ obeys the Ermakov equation [34]

$$\ddot{\sigma} + \omega^2\sigma = \frac{\hbar^2}{4m^2\sigma^3} + \frac{Ng}{4\sqrt{\pi}m\sigma^2} \tag{2}$$

(see the Supplemental Material [35], Sec. A, for details). When inserted into the Gaussian ansatz for ψ, this procedure yields the Gaussian wave function that best approximates the exact solution of the GPE. This approximation is exact for $g = 0$ and remains reasonably accurate for moderate interactions, as was shown for a Coulomb gas [32].

Quantum-classical analogy. We now introduce the quantum-classical analogy based on Nelson's stochastic quantization [13,36] (see the Supplemental Material [35], Sec. B). The latter stipulates that the Schrödinger equation is equivalent to a classical stochastic process governed by a first-order Langevin equation $\mathrm{d}x(t) = b(x(t),t)\mathrm{d}t + \mathrm{d}W$, where $\mathrm{d}x$ is the position increment, $\mathrm{d}t$ is the time step, and $\mathrm{d}W$ is a Wiener process with zero mean and correlations $\langle \mathrm{d}W(t)\mathrm{d}W(t')\rangle = 2D\mathrm{d}t\,\delta(t-t')$, with $D = \hbar/2m$ the quantum diffusion coefficient. The drift velocity $b(x,t)$ can be written in terms of the amplitude and phase of the wave function, $b(x,t) = \frac{\hbar}{m}\partial_x S(x,t) + D\partial_x \ln P(x,t)$.

When the wave function is Gaussian, as we have assumed earlier, the drift velocity is linear in x, and the Nelson stochastic equation can be written as

$$\mathrm{d}x = (\hbar/2m)[4\alpha(t) - \sigma^{-2}(t)]x\mathrm{d}t + \mathrm{d}W. \tag{3}$$

The above equation is identical to an overdamped Ornstein-Uhlenbeck (OU) process [37]

$$\mathrm{d}x = -\gamma^{-1}\bar{\kappa}(t)x\mathrm{d}t + \mathrm{d}W, \tag{4}$$

where $\bar{\kappa}(t)$ is the stiffness of a classical harmonic trap and γ is a drag coefficient that we include for dimensional consistency. Equations (3) and (4) become identical when the coefficients in front of the deterministic terms are the same. Equating these coefficients, one finds

$$\kappa(t) - \frac{Ng(t)}{4\sqrt{\pi}\sigma^3(t)} = \frac{\hbar^2}{2m\sigma^4(t)} + \frac{m}{\gamma}\dot{\bar{\kappa}}(t) - \frac{m}{\gamma^2}\bar{\kappa}^2(t) \tag{5}$$

(see the Supplemental Material [35], Sec. C). Equation (5) is the main element of the quantum-classical analogy, relating the classical stiffness $\bar{\kappa}$ to the quantum control parameters g and κ [12].

The variance $s(t)$ of the OU process (4) obeys

$$\frac{\mathrm{d}s}{\mathrm{d}t} = \frac{2}{\gamma}[D\gamma - \bar{\kappa}(t)s], \tag{6}$$

with equilibrium condition $\bar{\kappa}_{\mathrm{eq}} = D\gamma/s_{\mathrm{eq}}$. When Eq. (5) is satisfied the variance s is identical to the squared width σ^2 of the Gaussian wave function: $s(t) = \sigma^2(t)$. In other words, the approximate Gaussian solution of the GPE with time-dependent stiffness $\kappa(t)$ and interaction strength $g(t)$ is identical to the solution of a classical OU process with oscillator stiffness $\bar{\kappa}(t)$, provided κ, g, and $\bar{\kappa}$ satisfy Eq. (5). Hence, a BEC for which either $g(t)$ or $\kappa(t)$ (or both) are time dependent can be emulated by a classical stochastic process with variable stiffness $\bar{\kappa}(t)$.

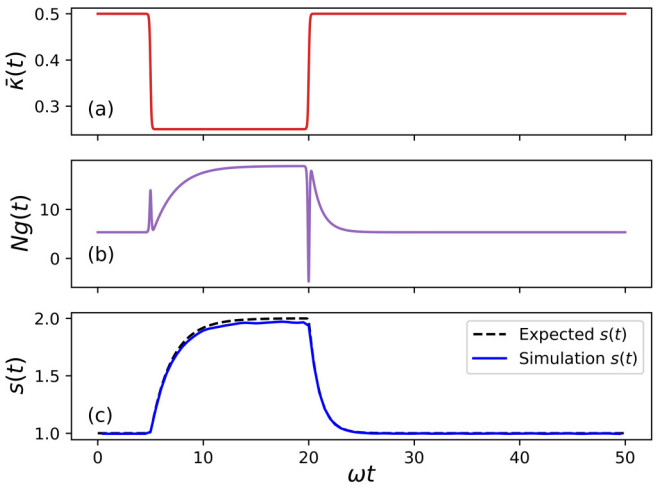


FIG. 1. (a) Steplike protocol on the classical stiffness $\bar{\kappa}(t)$ and (b) corresponding quantum $g(t)$ protocol computed from Eq. (5) (b). (c) Variance $s(t)$ obtained from Eq. (6) (black dashed line) and that computed from a numerical simulation of the GPE (black solid line) using the time-dependent interaction strength $g(t)$ shown in (b). Here s is expressed in units of $L_{\mathrm{HO}}^2 = \hbar/m\omega$, $\bar{\kappa}$ in units of $m\omega^2$, and g in units of $\hbar\omega L_{\mathrm{HO}}$.

In practice, in order to obtain the quantum protocol, one proceeds in three steps: (i) Fix the classical stiffness $\bar{\kappa}(t)$, (ii) solve Eq. (6) to obtain the variance $s(t)$, and (iii) use Eq. (5) to obtain either $\kappa(t)$ at fixed g or $g(t)$ at fixed κ. Finally, the GPE is solved numerically with the obtained quantum protocol $g(t)$ or $\kappa(t)$ and $\langle x^2\rangle = \int x^2|\psi|^2\mathrm{d}x$ is compared to the expected variance $s(t)$.

Example: Shortcut to adiabaticity. We search for a protocol that transitions the system from $s_i = 1$ to $s_f = 2$ (and backward) by acting only on the interaction strength $g(t)$, while the quantum stiffness κ remains constant. To do so, we assume a smoothed step function for the classical stiffness $\bar{\kappa}(t)$, as represented in Fig. 1(a). Using Eq. (5) with κ constant, we obtain the functional form of $g(t)$ shown in Fig. 1(b). Such a form is highly nontrivial, but nicely ensures the transition from $s_i = 1$ to $s_f = 2$ and backward, in a time of the order of $15\omega^{-1}$, i.e., about 2.5 oscillation periods of the trap potential, a significant improvement compared to an adiabatic (infinitely slow) protocol.

Directly injecting this protocol $g(t)$ into the GPE yields a result very similar to that of the theoretical model, with the variance reaching a stable plateau with minimal fluctuations [Fig. 1(c)]. The ability to steer the system back and forth between two equilibrium configurations, by acting on the interaction strength $g(t)$, foreshadows the possibility of devising quantum BEC engines, which will be addressed in the following paragraphs.

Optimal protocols. The protocol of Fig. 1 allows us to drive the system to a new equilibrium in a time corresponding to just a few trap periods. However, one can do even better by deriving an optimal protocol that minimizes the duration of the transition. In order to do so, we adopt the method illustrated in our earlier works [12,38]. We first change the independent variable from the time t to the variance s, using the transformation

$$t(s) = \int_{s_i}^{s} \frac{\mathrm{d}s}{\mathrm{d}s/\mathrm{d}t} = \int_{s_i}^{s} \frac{\gamma}{2} \frac{\mathrm{d}s}{D\gamma - \bar{\kappa}(s)}, \tag{7}$$

where we made use of Eq. (6). This transformation holds only if $s(t)$ is a monotonic function. For simplicity, we use the same symbol for a function of time, such as $\bar{\kappa}(t)$, and the corresponding function of the variance $\bar{\kappa}(s) \equiv \bar{\kappa}(t(s))$. Then we construct the cost functional to be minimized:

$$J[\bar{\kappa}, \bar{\kappa}'] = \int_{s_i}^{s_f} \left(\frac{1}{2} \frac{\gamma}{D\gamma - s\bar{\kappa}(s)} + \lambda f(s, \bar{\kappa}, \bar{\kappa}') + \mu |\bar{\kappa}'|^2 \right) \mathrm{d}s. \tag{8}$$

The first term represents the total duration of the protocol $\Delta t = \int_0^{t_f} \mathrm{d}t = \frac{\gamma}{2} \int_{s_i}^{s_f} \mathrm{d}s/[D\gamma - \bar{\kappa}(s)s]$, the second term is an arbitrary cost to be defined later, and the last term limits the gradient of the stiffness. Here λ and μ are Lagrange weights that modulate the relative importance of each term. Their choice determines, for instance, the duration Δt of the protocol.

The choice of the cost function $f(s, \bar{\kappa}, \bar{\kappa}')$ is dictated by the quantity that the user wishes to optimize alongside the duration of the protocol. Following our earlier work [12], we choose to minimize the (squared) phase of the wave function $\alpha(t) = \frac{m}{2\hbar} \frac{\dot{\sigma}}{\sigma}$. This choice yields the cost function $f(s, \bar{\kappa}, \bar{\kappa}') = \frac{m^2}{8\gamma\hbar^2}(D\gamma - s\bar{\kappa})/s^2$ (see the Supplemental Material [35], Sec. D). Then the Euler-Lagrange equation for the total cost functional (8) reads

$$2\mu \frac{\mathrm{d}^2\bar{\kappa}}{\mathrm{d}s^2} = \frac{\gamma s}{(D\gamma - s\bar{\kappa})^2} - \lambda \frac{m^2}{8\gamma\hbar^2 s}. \tag{9}$$

Solving Eq. (9) with boundary conditions at equilibrium $\bar{\kappa}_{i,f} = D\gamma/s_{i,f}$ yields a protocol with optimal trade-off between total duration, phase, and gradient of the stiffness. Such a trade-off can be modulated through the Lagrange weights λ and μ. We note that, for an adiabatic process, the phase is $\alpha(t) \approx 0$, because all quantities vary infinitely slowly. Hence, our choice to minimize $|\alpha|$ is tantamount to constructing protocols that are "adiabatically optimal," i.e., they are as close as possible to an adiabatic process compatibly with a finite duration.

Figure 2 shows three optimal g-protocols that transfer the variance from $s_i = 1$ to $s_f = 2$, for $\lambda = 8$ and three values of μ, corresponding to different durations. The evolution of the variance in Fig. 2(a) has been obtained by direct numerical solution of the GPE with the optimal protocol $g(t)$ shown in Fig. 2(b). In order to highlight the remarkable stability of the solutions, the simulations have been extended beyond the end of the protocol, keeping $g(t)$ constant and equal to its final value. Such optimal protocols lead to a transition time Δt that is significantly shorter than one oscillation period of the trap potential, $T = 2\pi/\omega$, whereas for the simple step of Fig. 1 we had $\Delta t \approx 2.5T$. Only for the shortest protocol does $g(t)$ take some negative values, which would be difficult, but not impossible, to realize in practice.

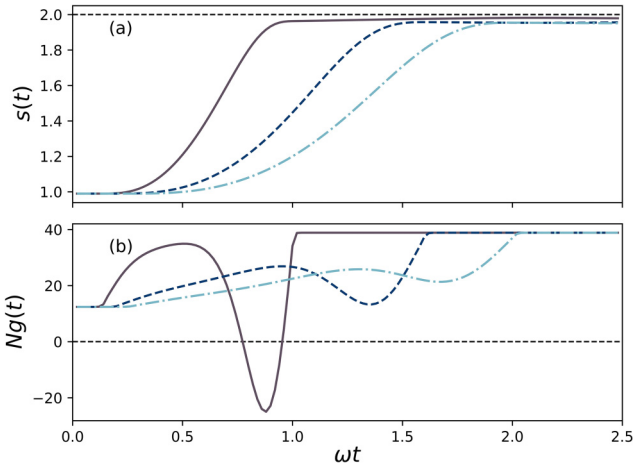


FIG. 2. Optimal protocol with $\lambda = 8$ and three values of the weight $\mu = 0.1$ ($\omega\Delta t = 1.06$, purple solid line), $\mu = 0.5$ ($\omega\Delta t = 1.68$, dark blue dashed line), and $\mu = 1$ ($\omega\Delta t = 2.11$, light blue dot-dashed line), where Δt is the duration of the protocol. (a) Variance computed from the GPE using the optimal protocol $g(t)$ shown in (b). The runs are continued after the end of the protocols, keeping g constant and equal to its final value, in order to highlight their stability. The variance s is expressed in units of $L_{\mathrm{HO}}^2 = \hbar/m\omega$ and g in units of $\hbar\omega L_{\mathrm{HO}}$.

Optimal Feshbach engines. Here we make full use of Eq. (5) to devise efficient BEC cycles. This equation enables one to convert the BEC dynamics, governed by the GPE with varying stiffness $\kappa(t)$ and/or interaction strength $g(t)$, into a classical stochastic process where only the stiffness $\bar{\kappa}(t)$ is time dependent.

In the simulation results, time is expressed in terms of the reference frequency $\omega_0/2\pi = 17.5$ Hz ($\omega_0^{-1} \approx 9.1$ ms), the variance in units of $L_{\mathrm{HO}}^2 = \hbar/m\omega_0$, the stiffness in units of $m\omega_0^2$, and g in units of $\hbar\omega_0 L_{\mathrm{HO}}$. For instance, for lithium atoms ^{7}Li [39], one has $m = 1.17 \times 10^{-26}$ kg, yielding $L_{\mathrm{HO}} \approx 3.6$ μm.

In Fig. 3 we consider an engine whose unit cycle *ABCDA* is made of four strokes that each minimize the phase α of the BEC wave function, thus making the overall cycle as close as possible to an adiabatic one, but with finite duration. During each stroke, either κ is modulated at constant g (steps *AB* and *CD*), or g is varied at constant κ (steps *BC* and *DA*). Such an engine was recently realized experimentally with a 3D isotropic BEC constituted of ^{7}Li atoms [39]. Our approach could be easily extended to that geometry by using a spherically symmetric GPE [40,41]. A 3D nonisotropic case with Coulomb nonlinearity was considered in [33].

We ran this quantum engine for a total of four cycles to highlight its remarkable stability. The bottom panel of Fig. 3 shows the evolution of $s(t)$ deduced from our optimization procedure (dashed line), together with the variance $\langle x^2 \rangle$ obtained from the numerical solution of the GPE, showing excellent agreement. The GPE is run some time after the end of the last cycle, with constant g and κ, in order to highlight the robustness of the final state. In the Supplemental

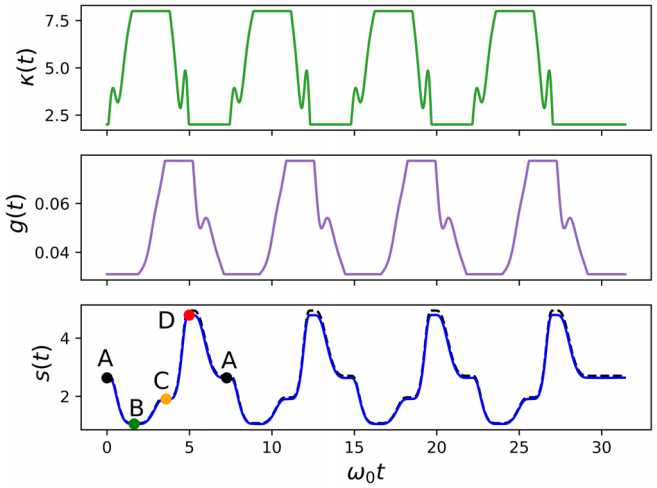


FIG. 3. Four cycles of an optimal quantum engine for a BEC consisting of $N = 2000$ atoms. Each cycle alternates between κ transitions and g transitions. The top and middle panels show the evolutions of $\kappa(t)$ and $g(t)$. The bottom panel shows the variance expected from the theoretical protocols (black dashed line) and computed from simulations of the GPE (blue solid line). The full *ABCDA* cycle is a sequence of four strokes: $\kappa_i \to \kappa_f$ at constant g_i (AB), $g_i \to g_f$ at constant κ_f (BC), $\kappa_f \to \kappa_i$ at constant g_f (CD), and $g_f \to g_i$ at constant κ_i (DA). Here $\kappa_i = 2$, $\kappa_f = 8$ (hence $\omega_i = \sqrt{2}$, $\omega_f = \sqrt{8}$), $g_i = 0.031$, and $g_f = 0.0775$, expressed in the normalized units defined in the text. The initial and final variances are computed from Eq. (5) at steady state. The Lagrange weights are $\lambda = 0.01$ (for all strokes) and $\mu_{AB} = 1$, $\mu_{BC} = 4$, and $\mu_{CD} = \mu_{DA} = 0.5$.

Material [35], Sec. E, we show the reverse cycle *ADCBA*, which is just as stable as the forward one. The observed reversibility is a further signature that the cycle mimics an adiabatic one, but with finite duration. Finally, in Fig. 4, the same cycle is repeated 32 times, without any noticeable loss of stability.

Power and efficiency. The quantum engine studied above differs from ordinary thermal engines [42,43] inasmuch as it does not use heat to produce work; instead, it converts one type of energy into another. In our case, it converts the

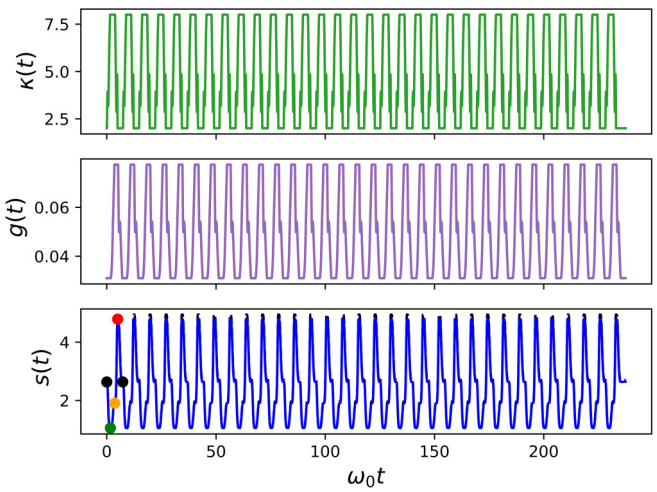


FIG. 4. Same as Fig. 3 but for 32 repetitions of the cycle.

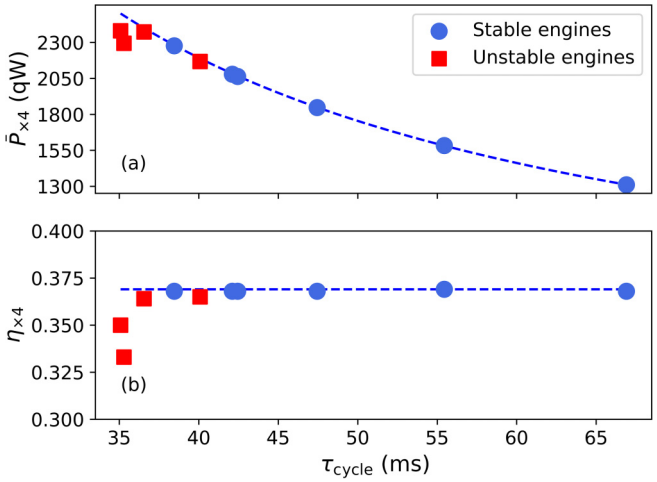


FIG. 5. (a) Total power and (b) efficiency, both averaged over four cycles, versus cycle time. The blue circles refer to stable cycles (irreversible work $W_{\rm irr} \ll \Delta_{IJ}$) and the red squares to unstable cycles. Power is measured in quectowatts (1 qW $= 10^{-30}$ W). The dashed lines show the ideal results for $W_{\rm irr} = 0$.

magnetic energy needed to modulate g through the Feshbach resonance [17,19] into mechanical work. Two important quantities to assess the quality of a cycle are its efficiency η and the total delivered power P per cycle, defined respectively as [25]

$$\eta = -\frac{W_{AB} + W_{CD}}{W_{BC}}, \qquad P = -\frac{W_{AB} + W_{CD}}{\tau_{\rm cycle}},$$

where $\tau_{\rm cycle}$ is the total cycle time and W_{IJ} is the work done on the BEC during stroke IJ of the cycle. If I and J are stationary states, then W_{IJ} is equal to the energy difference $\Delta_{IJ} \equiv E_J - E_I$, where $E_{I,J}$ are steady-state energies computed from the GPE. By convention, $W > 0$ when the system gains energy. Note that P is an extensive quantity that depends on the number N of atoms. If the target state is not stationary, then some irreversible work appears: $W_{IJ} = \Delta_{IJ} + W_{\rm irr}$. We call an engine stable when $W_{\rm irr} \approx 0$ after many cycles and unstable when $W_{\rm irr} \neq 0$.

The efficiency and power for several quantum engines are plotted in Fig. 5 as a function of the cycle time. Power increases at shorter cycle times, as expected. Below a certain critical value of $\tau^*_{\rm cycle}$, some irreversible work appears and the cycle loses both power and efficiency. It can be checked that $\tau^*_{\rm cycle} \approx 2\pi/\omega_i$, which is the longest period of the trap harmonic potential. The extracted power is considerably larger than that reported in recent experiments [39], while the cycle time is shorter. Despite differences in geometry (isotropic vs cigar shaped) and regime (Thomas-Fermi vs diluted), these results suggest that our optimal control approach could significantly enhance the output power.

Conclusion. In this Letter we have developed a comprehensive strategy to obtain optimally efficient quantum cycles for an engine based on a trapped BEC. The cycle is based on alternate strokes that modify either the trap stiffness at constant interaction strength (tuned via the Feshbach resonance) or the interaction strength at constant stiffness. Such engines, which convert magnetic energy into mechanical energy and vice versa, have recently been

realized experimentally [39]. A variational approach enabled us to optimize each stroke of the cycle by minimizing a user-defined cost functional. The same technique may apply to other atomic gases, such as Fermi-Bose mixtures at the BEC-BCS crossover [44,45]. The present findings may have potential applications to atomtronics [46], i.e., the quantum technology of matter-wave circuits that coherently guide ultracold atomic gases, and to hybrid systems where ultracold atoms are coupled to micro- and nanomechanical oscillators [47].

Moreover, our work illustrates a general procedure to construct optimal protocols for systems governed by a nonlinear Schrödinger equation (NLSE): (i) Posit a Gaussian ansatz for the wave function, (ii) obtain an approximate solution of the NLSE through a variational method, (iii) derive the classical stochastic analog (Ornstein-Uhlenbeck) using Nelson's method, (iv) define an appropriate cost functional to be minimized, and finally (v) solve the corresponding Euler-Lagrange equation to obtain the optimal protocol. This versatile approach provides an opportunity for future applications in fields as varied as nonlinear optics, quantum fluids, and quantum plasmas.

Acknowledgments. This work of the Interdisciplinary Thematic Institute QMat, as part of the ITI 2021–2028 program of the University of Strasbourg, CNRS, and Inserm, was supported by IdEx Unistra (Grant No. ANR 10 IDEX 0002) and by the SFRI STRAT'US project (Grant No. ANR 20 SFRI 0012) and EUR QMAT Grant No. ANR-17-EURE-0024 under the framework of the French Investments for the Future Program.

Data availability. There are no publicly available research data or software supporting this Letter. Requests for further information or data should be sent to the authors.

[1] J. I. Cirac and P. Zoller, Goals and opportunities in quantum simulation, Nat. Phys. **8**, 264 (2012).

[2] S. Deffner and S. Campbell, *Quantum Thermodynamics: An Introduction to the Thermodynamics of Quantum Information* (Morgan & Claypool Publishers, 2019).

[3] E. Torrontegui, S. Ibáñez, S. Martínez-Garaot, M. Modugno, A. Del Campo, D. Guéry-Odelin, A. Ruschhaupt, X. Chen, and J. G. Muga, in *Advances In Atomic, Molecular, and Optical Physics*, edited by E. Arimondo, P. R. Berman, and C. C. Lin (Elsevier, Amsterdam, 2013), Vol. 62, pp. 117–169.

[4] D. Guéry-Odelin, A. Ruschhaupt, A. Kiely, E. Torrontegui, S. Martínez-Garaot, and J. G. Muga, Shortcuts to adiabaticity: Concepts, methods, and applications, Rev. Mod. Phys. **91**, 045001 (2019).

[5] J. Li, K. Sun, and X. Chen, Shortcut to adiabatic control of soliton matter waves by tunable interaction, Sci. Rep. **6**, 38258 (2016).

[6] E. Torrontegui, S. Ibáñez, X. Chen, A. Ruschhaupt, D. Guéry-Odelin, and J. G. Muga, Fast atomic transport without vibrational heating, Phys. Rev. A **83**, 013415 (2011).

[7] A. del Campo, Shortcuts to adiabaticity by counterdiabatic driving, Phys. Rev. Lett. **111**, 100502 (2013).

[8] M. V. Berry, Transitionless quantum driving, J. Phys. A: Math. Theor. **42**, 365303 (2009).

[9] S. Masuda and K. Nakamura, Fast-forward of adiabatic dynamics in quantum mechanics, Proc. R. Soc. A **466**, 1135 (2010).

[10] C. A. Plata, A. Prados, E. Trizac, and D. Guéry-Odelin, Taming the time evolution in overdamped systems: Shortcuts elaborated from fast-forward and time-reversed protocols, Phys. Rev. Lett. **127**, 190605 (2021).

[11] D. Raynal, T. de Guillebon, D. Guéry-Odelin, E. Trizac, J.-S. Lauret, and L. Rondin, Shortcuts to equilibrium with a levitated particle in the underdamped regime, Phys. Rev. Lett. **131**, 087101 (2023).

[12] V. Hardel, G. Manfredi, P.-A. Hervieux, and R. Goerlich, Shortcuts to adiabaticity in harmonic traps: A quantum-classical analog, Phys. Rev. E **110**, 054138 (2024).

[13] E. Nelson, Derivation of the Schrödinger equation from Newtonian mechanics, Phys. Rev. **150**, 1079 (1966).

[14] Y. Castin, Bose-Einstein condensates in atomic gases: Simple theoretical results, in *Coherent Atomic Matter Waves. Les Houches - Ecole d'Ete de Physique Theorique*, edited by R. Kaiser, C. Westbrook, and F. David (Springer, Berlin, Heidelberg, 2001), Vol 72.

[15] F. Dalfovo, S. Giorgini, L. P. Pitaevskii, and S. Stringari, Theory of Bose-Einstein condensation in trapped gases, Rev. Mod. Phys. **71**, 463 (1999).

[16] Y. Kagan, E. L. Surkov, and G. V. Shlyapnikov, Evolution and global collapse of trapped Bose condensates under variations of the scattering length, Phys. Rev. Lett. **79**, 2604 (1997).

[17] G. Roati, M. Zaccanti, C. D'Errico, J. Catani, M. Modugno, A. Simoni, M. Inguscio, and G. Modugno, ^{39}K Bose-Einstein condensate with tunable interactions, Phys. Rev. Lett. **99**, 010403 (2007).

[18] C. D'Errico, M. Zaccanti, M. Fattori, G. Roati, M. Inguscio, G. Modugno, and A. Simoni, Feshbach resonances in ultracold ^{39}K, New J. Phys. **9**, 223 (2007).

[19] C. Chin, R. Grimm, P. Julienne, and E. Tiesinga, Feshbach resonances in ultracold gases, Rev. Mod. Phys. **82**, 1225 (2010).

[20] A. del Campo, Frictionless quantum quenches in ultracold gases: A quantum-dynamical microscope, Phys. Rev. A **84**, 031606(R) (2011).

[21] J.-F. Schaff, X.-L. Song, P. Capuzzi, P. Vignolo, and G. Labeyrie, Shortcut to adiabaticity for an interacting Bose-Einstein condensate, Europhys. Lett. **93**, 23001 (2011).

[22] K. Brandner, M. Bauer, M. T. Schmid, and U. Seifert, Coherence-enhanced efficiency of feedback-driven quantum engines, New J. Phys. **17**, 065006 (2015).

[23] M. Beau, J. Jaramillo, and A. Del Campo, Scaling-up quantum heat engines efficiently via shortcuts to adiabaticity, Entropy **18**, 168 (2016).

[24] F. Wu, L. Chen, F. Sun, C. Wu, F. Guo, and Q. Li, Quantum degeneracy effect on performance of irreversible Otto cycle with ideal Bose gas, Energy Convers. Manage. **47**, 3008 (2006).

[25] J. Li, T. Fogarty, S. Campbell, X. Chen, and T. Busch, An efficient nonlinear Feshbach engine, New J. Phys. **20**, 015005 (2018).

[26] T. Keller, T. Fogarty, J. Li, and T. Busch, Feshbach engine in the Thomas-Fermi regime, Phys. Rev. Res. **2**, 033335 (2020).

[27] V. V. Nautiyal, R. S. Watson, and K. V. Kheruntsyan, A finite-time quantum Otto engine with tunnel coupled one-dimensional Bose gases, New J. Phys. **26**, 063033 (2024).

[28] J. A. Estrada, F. Mayo, A. J. Roncaglia, and P. D. Mininni, Quantum engines with interacting Bose-Einstein condensates, Phys. Rev. A **109**, 012202 (2024).

[29] C. Mishra, T. Busch, and T. Fogarty, Shortcuts to adiabaticity in anisotropic Bose-Einstein condensates, New J. Phys. **27**, 033009 (2025).

[30] C. Fort, L. Fallani, V. Guarrera, J. E. Lye, M. Modugno, D. S. Wiersma, and M. Inguscio, Effect of optical disorder and single defects on the expansion of a Bose-Einstein condensate in a one-dimensional waveguide, Phys. Rev. Lett. **95**, 170410 (2005).

[31] G. Manfredi and P.-A. Hervieux, Fidelity decay in trapped Bose-Einstein condensates, Phys. Rev. Lett. **100**, 050405 (2008).

[32] F. Haas, G. Manfredi, P. K. Shukla, and P.-A. Hervieux, Breather mode in the many-electron dynamics of semiconductor quantum wells, Phys. Rev. B **80**, 073301 (2009).

[33] J. Hurst, K. Lévêque-Simon, P.-A. Hervieux, G. Manfredi, and F. Haas, High-harmonic generation in a quantum electron gas trapped in a nonparabolic and anisotropic well, Phys. Rev. B **93**, 205402 (2016).

[34] H. R. Lewis, Classical and quantum systems with time-dependent harmonic-oscillator-type Hamiltonians, Phys. Rev. Lett. **18**, 510 (1967).

[35] See Supplemental Material at http://link.aps.org/supplemental/10.1103/ymmx-hskw for further details on the variational method (Sec. A), Nelson's stochastic quantization (Sec. B), the quantum-classical analogy (Sec. C), the cost functional (Sec. D), and the reverse cycle (Sec. E).

[36] G. Bacciagaluppi, Nelsonian mechanics revisited, Found. Phys. Lett. **12**, 1 (1999).

[37] G. E. Uhlenbeck and L. S. Ornstein, On the theory of the Brownian motion, Phys. Rev. **36**, 823 (1930).

[38] Y. Rosales-Cabara, G. Manfredi, G. Schnoering, P.-A. Hervieux, L. Mertz, and C. Genet, Optimal protocols and universal time-energy bound in Brownian thermodynamics, Phys. Rev. Res. **2**, 012012(R) (2020).

[39] E. Q. Simmons, R. Sajjad, K. Keithley, H. Mas, J. L. Tanlimco, E. Nolasco-Martinez, Y. Bai, G. H. Fredrickson, and D. M. Weld, Thermodynamic engine with a quantum degenerate working fluid, Phys. Rev. Res. **5**, L042009 (2023).

[40] G. Manfredi, P.-A. Hervieux, and F. Haas, Variational approach to the time-dependent Schrödinger-Newton equations, Classical Quantum Grav. **30**, 075006 (2013).

[41] F. Tanjia, J. Hurst, P.-A. Hervieux, and G. Manfredi, Plasmonic breathing modes in C_{60} molecules: A quantum hydrodynamic approach, Phys. Rev. A **98**, 043430 (2018).

[42] R. S. Watson and K. V. Kheruntsyan, Quantum many-body thermal machines enabled by atom-atom correlations, SciPost Phys. **18**, 190 (2025).

[43] S. Campbell, I. D'Amico, M. A. Ciampini, J. Anders, N. Ares, S. Artini, A. Auffèves, L. B. Oftelie, L. P. Bettmann, M. V. S. Bonança, T. Busch, M. Campisi, M. F. Cavalcante, L. A. Correa, E. Cuestas, C. B. Dag, S. Dago, S. Deffner, A. Del Campo, A. Deutschmann-Olek, *et al.*, Roadmap on quantum thermodynamics, Quantum Sci. Technol. **11**, 012501 (2026).

[44] J. Koch, K. Menon, E. Cuestas, S. Barbosa, E. Lutz, T. Fogarty, T. Busch, and A. Widera, A quantum engine in the BEC–BCS crossover, Nature (London) **621**, 723 (2023).

[45] K. Menon, T. Busch, and T. Fogarty, Leveraging quantum statistics to enhance heat engines, Quantum Sci. Technol. **10**, 045039 (2025).

[46] L. Amico, D. Anderson, M. Boshier, J.-P. Brantut, L.-C. Kwek, A. Minguzzi, and W. von Klitzing, *Colloquium*: Atomtronic circuits: From many-body physics to quantum technologies, Rev. Mod. Phys. **94**, 041001 (2022).

[47] D. Hunger, S. Camerer, M. Korppi, A. Jöckel, T. W. Hänsch, and P. Treutlein, Coupling ultracold atoms to mechanical oscillators, C. R. Phys. **12**, 871 (2011).